The lifetime and future of double clusters: Why there are so few observed binary star clusters

Mira Håkansson

Division of Astrophysics
Department of Physics

LUND UNIVERSITY

2024–EXA234

Degree project of 15 higher education credits
June 2024

Supervisor: Ross Church

Division of Astrophysics
Department of Physics
Box 118
SE-221 00 Lund
Sweden

Abstract

Binary open star clusters within the Milky Way are rare. Only 14 candidates have been confirmed with new Gaia data (Song et al. 2022). The number of binary clusters expected to form from stellar aggregates in the Milky Way is likely more than five times higher than this (Darma et al. 2021), (Kharchenko et al. 2012). Using the N-body simulation program NBODY6 we simulate two known open clusters; the binary system of h and χ Persei over time. We want to evaluate the effect that changing the eccentricity of orbit of the clusters has on their life-time. The limit of the life-time for a perfectly circular orbit was at most 200 million years (Myrs), meaning that astronomers only have this window to discover the binary star clusters. The reason for the unexpectedly low number of observational data is then explained by the low life-time of clusters of the kind of h and χ Persei, the most famous and oldest known to man. The merging of the clusters produce a stable cluster which evaporates with a slightly lower rate than an isolated cluster for the beginning of its life, but the life-time of the merger product is not affected.

Popular Science Description

There are few things that sparks one's imagination quite like outer space. It extends for billions of light-years in all directions around Earth, containing everything that has ever existed, all of it produced at the same time 13.8 billion years ago in the Big Bang. Structures such as stars, star clusters, galaxies and galaxy clusters have evolved naturally over billions of years as a result of gravity. Cosmology is the study of the history of the Universe and how these structures were formed, and since we exist in a certain time and place in the Universe, our knowledge and research is limited. Scientists point telescopes out into space and gather as much data as possible, and each day work on improving methods and instruments of observation to be able to gather new information or resolve uncertainties in the data we receive from the telescopes.

It's only in recent times that computers have been utilized to create models of objects and structures of the Universe, which has significantly altered the way we perform research. For example, using a set of data belonging to a star cluster based on actual observations, we can simulate the cluster's evolution over time and how the many initial parameters such as mass, velocity, number of stars, and potential nearby galaxies affect its evolution. Different models are produced using different simplifications applied to the forces which govern the cluster. We use these models in unison with models of other structures, to gain an understanding of what the universe could possibly look like in the future. One can also use the models backwards, in a kind of identification process. Say that we simulate a cluster over 100 million years (Myrs). Assume it's a known cluster which we have observed to have a specific mass and hosts 100 000 stars, with a certain orbit around the galaxy. After the 100 Myrs have passed, we now have new data for the cluster from the simulation. The cluster might have lost some stars, they now might have different orbits relative to each other, and the cluster as a whole might be more compact, etc. If we now find a cluster in the galaxy which displays these exact properties we could, based on our previous simulations, expect the cluster to have looked a certain way 100 Myrs in the past.

The computing power needed to simulate problems like these could easily be overlooked. To simulate how the stars within the cluster will behave, we need to take into account the force between each and every star. That is, the first star and all the other N-1 stars, and then the second star, and all the other N-1 stars, and so on. This is an operation on the scale of N^2 calculations. In my project I will be simulating and analyzing the evolution of 2 gravitationally bound star clusters, namely a double star cluster, consisting of NGC869 and NGC884. I will do this by utilizing a numerical simulation program and compare how the different inputs will affect the star clusters' evolution. The reason for doing this project is a discrepancy in the amount of predicted fraction of binary star clusters and the number of observed binary star clusters. Could it be that the model for binary star cluster formation is faulty or is there another explanation for the low number of observed binary clusters?

Contents

Chapter 1

Introduction

Star clusters have mesmerized humans for thousands of years. For instance, findings in the Lascaux cave from circa 17 000 BC (Rappenglück 1999) suggest they had observed the open cluster today known as Pleiades. Today, star clusters play a crucial role in astrophysical research and studying these celestial objects is of interest to many branches within the field. At the heart of research in astronomy lies cosmology, where galaxy evolution is one of the many remaining mysteries. An approach to understanding galaxy evolution, chemical composition and distances within them is the study of the formation and life of the star clusters within them. Star clusters also play a crucial role in research on stellar formation and evolution, as well as determining the ages of stellar populations (Pietrzynski & Udalski 2000). Young clusters can give clues surrounding stellar formation and evolution, whilst old clusters can grant insight into the past dynamical evolution of our galaxy (Cantat-Gaudin & Anders, F. 2020) which is difficult to study since it happens on the timescale of billions of years.

1.1 Star clusters

To describe star clusters, I adopt a definition from (Krause et al. 2020) which is very simple. A star cluster must contain at least 12 stars and not be dark matter-dominated. Star clusters are divided into two subgroups, open clusters and globular clusters. The distinction is mainly based on their visual appearance. Globular clusters have globe-like shape and a central region of higher density of stars. Open star clusters appear as a collection of stars with no real shape. A visual representation can be seen in figure 1.2. The clusters of interest in this project are both open clusters and lie in the Perseus arm of the Milky Way. A map can be found in figure 1.1.

Observational data of star clusters only provide snapshots of the clusters in time, and we would like to study the evolution of these clusters over time. To do this we need to use simulations to complement the data. In this study, we will try to understand how different initial conditions can affect the evolution of star clusters and what this could mean for

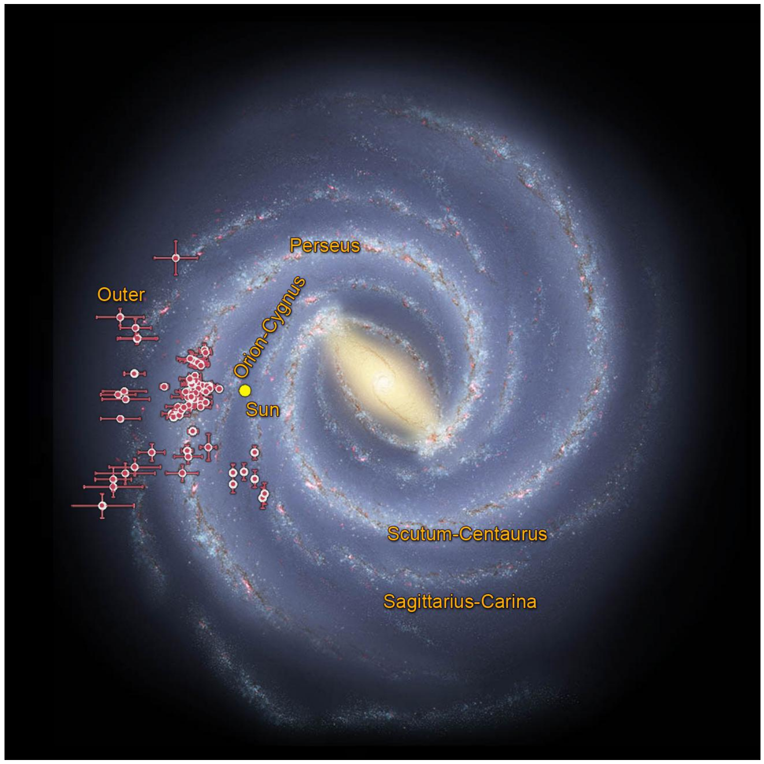

Figure 1.1: Map of the Milky Way, where the location of young star clusters embedded in dust is seen as well as the error on their data. We can also see the Perseus arm, where NGC869 and NGC884 are located. Image courtesy NASA/JPL-Caltech.

Figure 1.2: Visual representation of a globular cluster on the left and open cluster on the right.(Made in Inkscape).

the present data on binary star clusters, based on the double cluster h and χ Persei also named NGC869 and NGC884. By changing the input eccentricity for a simulation of the clusters over time we will investigate how this effects the merge time and the half-mass radius of the clusters. We will also compare the clusters within a binary system to an isolated cluster to see what effect being in a binary system has on the cluster.

1.2 Binary Star Clusters

NGC869 and NGC884, also known as h and χ Persei have until recently been the only known double cluster (Vázquez et al. 2010). A binary star cluster is a system of two gravitationally bound star clusters. They are gravitationally bound if their gravitational potential energy is larger than that of their kinetic energy. Previous studies on binary star clusters found that the frequency of star clusters exhibiting interaction with other clusters within the Large Magellanic Cloud (LMC)(Bhatia & Hatzidimitriou 1988) and the Small Magellanic Cloud(SMC) (Hatzidimitriou & Bhatia 1990), should be nearly 10%. Other, later studies have confirmed this number and raised it to around 12% (Pietrzynski & Udalski 2000). As recent as 2009, (de la Fuente Marcos & de la Fuente Marcos 2009) it was found that the fraction of open binary clusters in the Galactic disk is significant. They also conclude that the fraction of binary star clusters is likely at least 10%. However only around 17 percent of them survive as pairs beyond 25 million years (Myrs).

Thanks to the increase in precision of measurements since the launch of GAIA, more exact determination of whether two star clusters are bound have been done. Song et al. (2022) proposed that the number of detected binary open clusters in the GAIA data consist of 14 candidates. However, a global survey of the star clusters within the Milky Way (Kharchenko et al. 2012) found that out of the 871 candidates of star clusters, 642 of them were open clusters, 2 were globular clusters and 219 were nonexistent clusters, too faint to be recognized, or duplicate entries. The discrepancy of model to observation between the 642 open clusters and the 14 proposed binaries is obvious, with the fraction being only 2% instead of $\sim$ 10%. Ongoing research in the cataloging of star clusters mean that the membership status of both stars within clusters and whether the star clusters even are clusters update continuously (Cantat-Gaudin & Anders, F. 2020). In this thesis we will try to tackle one aspect as to why the number of predicted binary star clusters is much lower than the number of observed. By focusing on the life time and evolution of these binary star clusters, we want to find whether this could be limiting the observational data we have. Further research in the field could otherwise investigate the observational bias of star clusters, or whether the model for forming binary star clusters need to be modified.

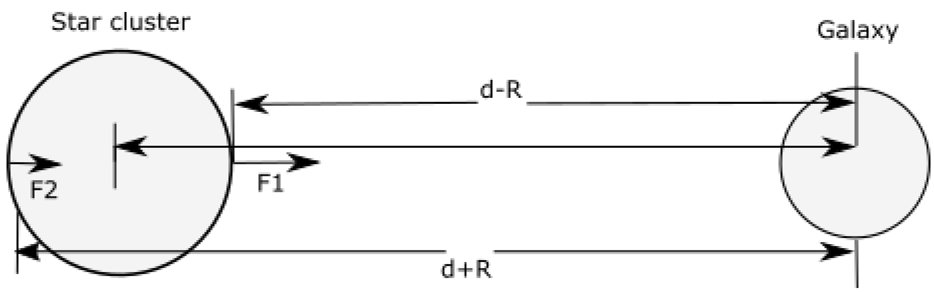

Figure 1.3: Visual representation of tidal force from a distant galaxy on a star cluster. F_1 is a stronger force than F_2 due to being closer to the object exerting the gravitational force.

1.3 Formation and Evolution of Star Clusters

Star cluster formation can be described as a three phase process (Krause et al. 2020). The interstellar medium of galaxies contains molecular clouds which host regions with highly varying densities. Turbulence in these clouds cause high density regions of the cloud to be short-lived while regions massive enough undergo gravitational collapse. While the gas of these high density regions collapses, it separates itself from the surrounding molecular cloud. Within the collapsing gas, proto-stars begin to form by the accretion of mass from the surrounding gas cloud. Another important part of the formation of star clusters is the role of stellar feedback. The stellar feedback is a process where the stars being formed within the cluster affect the neighboring stars. The effects are mainly due radiation, winds and supernovae (Krause et al. 2020). The stellar feedback clears the remaining gas and now the young star cluster has formed.

After the initial turbulent start to the cluster's life, the cluster is now a gas-less collection of gravitationally bound stars. They are governed by the gravitational force between each individual star. The exception to this is the tidal forces the cluster can experience from its host galaxy. They are called tidal forces since the galaxy pulls on the side of the cluster closer to it more than the side of the cluster furthest away. A visual representation can be seen in figure 1.3. On binary star clusters, this tidal force disrupts the orbit of them, and could pull them apart. This effect is more prominent for larger star clusters since the force difference on the two sides of the cluster becomes larger. Within the cluster, an individual stars energy per mass can be approximated as

$$\epsilon = \frac{E}{m} \approx \frac{1}{2}v^2 - \frac{GM_C}{r}, \tag{1.1}$$

with v being the velocity of the star, relative to the center of mass of the cluster, M_C being the mass of the cluster and r the distance between the star and the center of mass of the cluster. If the kinetic energy of the star is large enough, it will escape the gravitational potential of the star cluster and thus escape the cluster. For a star in cluster, the energy stated above is an approximation as the Plummer sphere has a softer gravitational potential, if we instead use the softer potential the potential is obtained by integrating the density distribution of the Plummer sphere. The potential at a distance r from the center of the cluster is then

$$\Phi = -\frac{m}{\sqrt{R^2 + \epsilon^2}}. \tag{1.2}$$

On top of the escapers from the cluster, over time the star clusters will undergo evaporation. The less stars in the cluster, the smaller the gravitational force between the center of mass(COM) and the individual stars. The weaker force means that the stars escape more easily, and thus the cluster evaporates quicker.

1.4 Half-mass radius

A way to measure the evaporation is to measure the half-mass radius of the cluster over time. The half-mass radius is calculated by summing the mass of the stars within the cluster nearest the center of mass, up until half of the total mass has been reached. The distance between the center of mass of the cluster and the last star within the half-mass limit will be the star cluster's half mass radius. An increasing half-mass radius will imply that the cluster is becoming larger and more loosely bound.

1.5 Formation of Binaries

Depending on the degree of internal substructure D, (Darma et al. 2021), within the molecular cloud that forms a stellar aggregate, the probability that a binary star cluster will be produced varies. The formation of binary star clusters have been modelled using N-body simulations of young star clusters with varying D (Darma et al. 2021). The results of these simulations are that from a star cluster, a binary can form if D is small. The fractal dimension parameter, D, quantifies the substructure degree of a star cluster within the range $D \in [0, 3]$. Lower values of D signify a clumpier cluster structure. The fraction of stellar aggregates which form binary star systems which survive for a substantial amount of time also depends on the environment. In the Large Magellanic Cloud(LMC) $\sim$ 90 percent of the formed binary star clusters survive past $t = 20$ Myrs, and $\sim$ 80 percent at $t = 50$ Myrs. Compared to when the binary star clusters are formed in the Milky Way, only about $\sim$ 30 percent remain after $t = 50$ Myrs, based on the simulations in Darma et al. (2021). The life-time of these binary clusters could depend on a number of parameters, for example the eccentricity of their orbit. The eccentricity is a measure on the shape of the orbit of the star clusters and a range of eccentricities are presented in figure 1.4. One aspect we want to research is the merging of the two clusters and if the merge time could be a reason for the sparse number of binaries we have found. The star clusters of NGC869 and NGC884 are the oldest known cluster with an age estimated to be between 15.13 Myrs and 17.78 Myrs (Song et al. 2022). and consist of 503 and 322 members, respectively. Studying their evolution with the use of real data and finding out whether they merge or not could give insight to the evolution of binary star clusters in general.

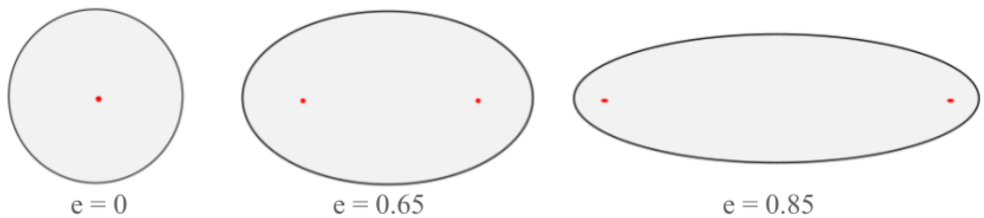

Figure 1.4: Visual representation of varying eccentricities, with the red dots representing the focal points.

1.6 Questions

The questions of importance in this thesis is how the dynamics of the clusters' evolution are affected by their initial conditions such as eccentricity of orbit, as well as the how the dynamics of a binary star cluster, and merge product, compares to a an isolated star cluster.

- How does a varying eccentricity of orbit affect the double cluster's life-time?
- How does an isolated star cluster's characteristics compare to that of a cluster within a binary?
- How does a cluster within a binary's half-mass radius change over time compared to a single cluster?

Chapter 2

Method

2.1 Simulations

2.1.1 Introduction to N-body problems

Star clusters are collections of gravitationally bound stars and we can simulate their collective behaviour by solving the corresponding equations of motion. We say that the cluster contains N stars, and calculate each star's gravitational pull on every other star. N-body problems require numerical solutions. In Sverre Aarseth's book (Aarseth 2003a) he discusses the numerical methods and how to develop algorithms for simulating gravitational systems. The direct approach is based on summation of forces and the gravitational force between particles can be written as

$$\ddot{\boldsymbol{r}}_{\boldsymbol{i}} = -G \sum_{j=1;j\neq i}^{N} \frac{m_j(\boldsymbol{r_i} - \boldsymbol{r_j})}{|\boldsymbol{r_i} - \boldsymbol{r_j}|^3} \tag{2.1}$$

This is the expression for the motion of a particle i in a system of N particles. Where the mass m_j is the mass of the other particles, r_i is the position of particle i and r_j is the position of particle j. In these N-body simulations we use G as 1 and scale the rest of the units in the expression, for convenience. $\ddot{\boldsymbol{r}}_{\boldsymbol{i}}$ is defined as the force per mass on the particle i. These equations are on the form of 3N second-order differential equations, or 6N first-order differential equations. The initial conditions for this problem is the mass, initial velocity and initial position for each individual particle. To solve these differential equations we use initial conditions for the mass, initial velocity and initial position for each particle.

The program we have chosen to work with is called NBODY6 and was developed by Sverre Arseth. The program is written in FORTRAN with around 55 000 rows of code (Aarseth 2003b). To utilize the numerical method, we leave the sets of continuous differential equations describing the motion of the stars within the cluster, for discrete difference equations. The difference equations take finite steps in time, and do the force calculation and sum for each of the stars for each . Since the computing power demanded to do this is large, steps are taken to ensure no unnecessary calculations are carried out and thus to ensure that the efficiency of the program is high.

Hermite Scheme

The program builds on what is called a Hermite scheme (Aarseth 2003a). The Hermite scheme is what makes it possible to carry out the time evolution of all stars at the same time, but with individual time-steps. It is based on splitting the stars into blocks so that a whole block is advanced at the same time, but not all stars are part of the block due for advancement. The reason we need individual time-steps like this is due to how gravity as a force behaves. A star near another star will have a much higher acceleration due to that star, than the rest of the cluster. Thus in the case of a binary star in orbit within the cluster, an approximation has to be made in order for the program to work smoothly. This is what is called a Kustaanheimo-Stiefel (KS) close encounter solution (Kustaanheimo et al. 1965). By using a coordinate change and adding a fourth coordinate to the problem as well as a perturbation to the motion of the two bodies interacting, we no longer need to account for integrating the orbit of the binary star. After these close encounter solutions have been carried out, the next step in the algorithm is to make changes to the force polynomials describing the complex behavior of the star cluster. Velocity and position of the stars are updated, and a block of particles is advanced.

Neighbours

Since the stars have the largest interaction with nearby stars, we can say that the star has a neighborhood of stars which primarily determine its motion, the rest are too far away. The Ahmad-Cohen method(Ahmad & Cohen 1973) is complex but briefly stated it combines two polynomials based on separate time-scales. One is the irregular force polynomial and one is the regular force polynomial

$$F = F_R + F_i. \tag{2.2}$$

Here we can sum over the n nearest particles, the neighbourhood, and add a combined contribution for the more distant particles instead of the full N. A neighborhood treatment is beneficial since it allows us to reduce the number of force summations we need to carry out. This is crucial in keeping the computing time low. The size of this neighborhood is modified after each integration cycle, once the whole N has been summed over.

Assumptions

Two types of assumptions are made in this project, ones that we make, and the ones that NBODY6 makes. Some of the assumptions in NBODY6 are required to ensure smooth simulations and to limit the run-time. Since we are simplifying the force of the distant stars when we use the neighborhood scheme, we are not accounting for the fact that these stars could alter the system. N-body simulations of stars are a chaotic system, meaning that a very small change could evolve into the system looking drastically different. An assumption that we choose in the input for the star clusters is that we do not take into account the tidal force on the clusters from the Milky Way. This effect could decrease the life-time of the star clusters or destabilize their orbits. The reason is that if the tidal force is accounted for, the clusters become de-coupled straight away, and since our aim is to study two bound clusters, this effect was chosen to be removed. We also wish to study how an isolated cluster evolves compared to a binary, and if the tidal force is then irrelevant for the single cluster, the comparison is accurate if the same is done for the double cluster.

The model assumes that the turbulent start of the clusters life, as described in section 1.5, has passed, since we base the data on the clusters with ages nearly 20 Myrs. In other words, we make the assumption that the star clusters have been stabilized and that formation of stars and the explosion of supernovae in the clusters have stopped. The gas within the cluster has also been cleared. This means that the physics of the cluster is no longer is as complex, nor is the internal processes within the cluster as chaotic as they were during the early formation of the cluster. This makes it easier to simulate the clusters.

Errors

There are three main types of errors when dealing with a simulation of this kind; We have round-off errors which come from the natural round-off which the computer makes when computing a value. The error is most significant when subtracting two nearly identical numbers, especially when the fractional difference is comparable to the computer's fractional precision in storing numbers. We also have errors which comes from transforming the continuous integral equations into discrete equation. This will produce an error of $O(dt^n)$ where n is determined from the scheme. The error of NBODY6-scheme produces an error of fifth order (Aarseth 2003a). We also have a deliberate algorithmic error which we caused by using the neighborhood treatment and ignoring the motion of the distant stars when advancing the stars in a block. This is deliberate to trade off numerical accuracy for speed of calculation.

2.1.2 Setup

The program has been developed to be used in a number of ways, one of which is for evolving star clusters over time. It distributes the mass, and position of the stars within the cluster according to a "Plummer Sphere" (Plummer 1911) which then determines the potential energy. A Plummer sphere is a description of a density distribution in space:

$$\rho(r) = \frac{3M}{4\pi a^3}\left(1 + \frac{r^2}{a^2}\right)^{-\frac{5}{2}}, \tag{2.3}$$

where M is the mass of the cluster, a is the Plummer radius, a scale factor.
We assume that the clusters are in virial equillibrium, thus the kinetic and potential energy

relates according to equation 2.4. The kinetic energy then determines the star's individual velocities which are assumed to follow a single Maxwell-Boltzmann distribution.

Once the inputs are sent into the program, the star clusters are initialized by the random seed determining the individual masses of the stars and their initial positions. The chosen virial radius determines the velocities of the stars and then the integration and time evolution takes place.

Inputs

The inputs of importance for the star clusters we are simulating include the eccentricity of their orbit, separation of clusters, scaling of the two clusters, number of members, and average mass of stars in the clusters. We use data presented in the paper by Song et al. (2022), as the initial conditions for these star clusters such as number of cluster members, average mass of stars belonging to the cluster and distance between the clusters, as given in the survey from (Song et al. 2022). When we run the simulations, the only parameter we change between runs is the eccentricity, varying it from 0.0 to 0.9 in steps of 0.1. The program initialises the clusters to begin at their orbit's furthest point of attraction, the apocenter. We choose the clusters to have $N = 500$ and $N = 300$. The program deals with both single stars as well as simulating the natural formation of binary stars, which are taken care of by the KS scheme discussed in section 2.1.1 under the *Hermite Scheme* paragraph. The mean mass of the stars is set to 0.5 solar masses, and the virial radius is set to 2 pc. The virial radius originates from the virial theorem which balances the kinetic energy and the potential energy of system:

$$2T + U = 0, \tag{2.4}$$

where U is the potential energy and T is the kinetic energy. For the clusters this means that we choose the virial radius, the distance at which this holds, to be 10% of their separation. We choose a relatively short virial radius to ensure that the initial clusters are clearly separated and stable enough to perform the simulations. The virial radius also relates to the parameter a, in the Plummer model of the clusters, equation 2.3, where it is given by

$$R_v = \frac{16a}{3\pi}. \tag{2.5}$$

The virial radius is a useful tool in setting up the clusters, and it also relates the energy E and mass M of the system (Heggie & Hut 2003),

$$R_v = -\frac{GM^2}{4E}. \tag{2.6}$$

We also input an energy error tolerance of $QE = 1$, and the program will stop if if $\frac{DE}{E} > 5QE$. In other words the energy of the system is not conserved. The reason to choose the energy error tolerance to be this large is simply to ensure the program runs for the time we choose, and we check the energy error at the end of each run to ensure accuracy.

Data output

The code has three main parts, input, integration and output. When the program is run using the input file, it creates and begins writing to a new file ”output”. Snapshots of the star clusters are also produced They consist of a text-file with a data row for each star in the clusters. The snapshot files are produced with a specific frequency specified in the input file. The integration cycle continues until a chosen time has been reached, or if the energy error becomes too large.

To test the accuracy of our simulation one can compare the total energy of the system before and after the simulation. The program does this automatically with the allowed energy error tolerance being one of the inputs. If this differs a lot, we do not follow the laws of conserved energy and angular momentum, and the program automatically interrupts the simulation. The energy of the system can be written as

$$E = \sum_{i=1}^{N} \frac{1}{2} m_i |\mathbf{v}_i|^2 - \sum_{i=1}^{N} \sum_{j=i+1}^{N} \frac{G m_i m_j}{|\mathbf{r}_i - \mathbf{r}_j|}$$

and the total angular momentum of the system can be written as

$$\mathbf{J} = \sum_{i=1}^{N} m_i \mathbf{r}_i \times \mathbf{v}_i.$$

Chapter 3

Results

3.1 Analysis

To analyze the data, a script was written in python and utilized. As it is impossible prior to analysis to determine which cluster a star belongs to, we iterate membership of all of the stars for each time-step. We determine each of their kinetic and potential energy (equation 1.1) in relation to both cluster's centers of mass, and determine which cluster the star is most bound to, if bound to any. Since it is possible for the stars to have been accelerated enough to escape the gravity of both cluster, these stars are labelled escapers and not used during the next iteration and calculation. The iteration continues until the number of stars in cluster 1 and cluster 2 converges. We plot the clusters over time using different colors for the different clusters as well as the separation between the centers of mass. We define that the clusters have merged once the distance between them is below a certain distance, and we check that this agrees with the figures, where we can clearly see if all the stars belong to the same cluster. If the clusters merge they all belong to the same cluster and a merge time is recorded. A flow chart describing the process is found in figure 3.1.

3.2 Time Evolution

We run the simulations changing only the input eccentricity of orbit for the two clusters. The output files have been analyzed using a python script, enabling us to determine cluster membership of the stars, as well as plotting them over time. A script for calculations such as the distance between the centers of mass, and the half mass radius was also made. A typical system is presented first, and then how the simulations change when varying the eccentricity is compared to this.

Simulations were also made with varying input random seed, but found that the simulations did not change and quantities such as merge time were too little to be of any significance. The runs are presented in table 3.1.

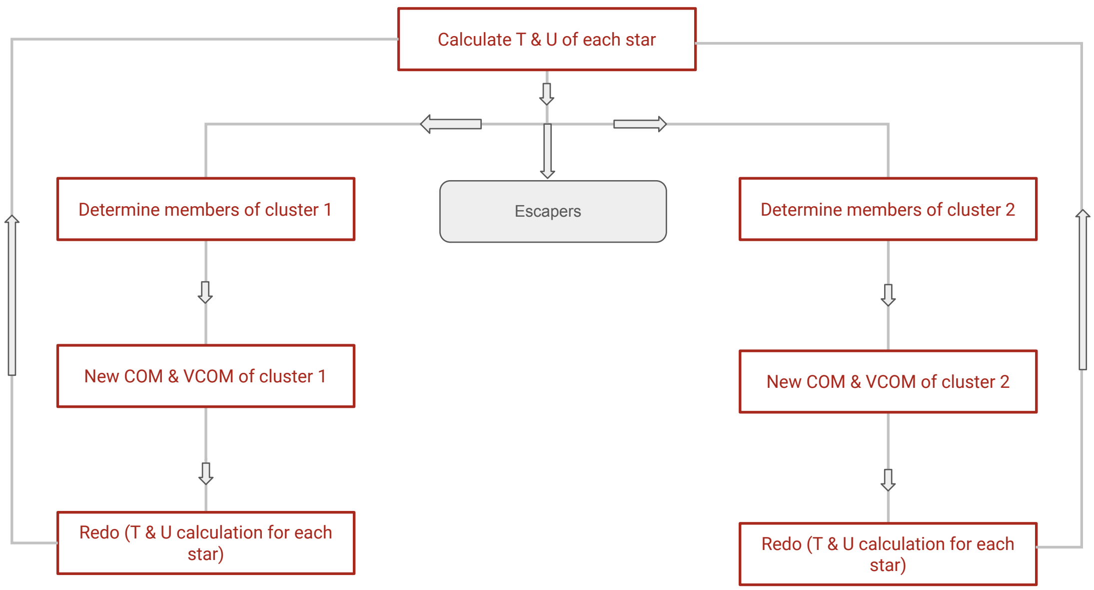

Figure 3.1: Flow chart describing the algorithm for membership determination.

Random seed	Eccentricity
10000	0.5
20000	0.5
30000	0.5
40000	0.5

Table 3.1: Simulations done with varying random seed.

The selected results shown in the text represent the data from the simulations. In figure 3.2 we see the evolution of a typical system of a single cluster over the full run-time. We see that the cluster becomes less dense over time. The half mass radius over time of this single cluster simulation can be found in figure 3.8.

In the figure 3.3, we present the case of a circular orbit. The clusters orbit each other and at 100 Myrs they seem to have completed a quarter of an orbit. They are somewhat disrupted, as their stars begin to spread out and escape the clusters. In the following time-steps we see the clusters less dense and more spread out, and the merge product seen at 380 Myrs is significantly less dense than the clusters in the first snapshot at $t = 0$.

We also present the evolution of two eccentricities, 0.1 and 0.5 next to each other in figure 3.4. We see that for the low eccentricity of 0.1, the clusters merge at 240 Myrs. When comparing to the eccentricity of 0.5, the merge time is less than half of this, 160 Myrs. At the same point in time, 140 Myrs, we see that the larger eccentricity clusters are much closer to each other, and also are later in their orbital phase.

The clusters with eccentricity 0.5 merge at 160 Myrs, however if we look closer at the next snapshot in figure 3.5, we see that we can still distinguish features of the separate clusters within the merge product. Even though they are gravitationally bound to a single center of mass, their internal structure still remains. This is less prominent in the merge product of the cluster with eccentricity 0.1 in the comparison, figure 3.4.

Figures for the evolution over time for a cluster with a high eccentricity of $e = 0.8$ is included in figure 3.6, as well as a plot for the separation between these clusters over time. We see that the clusters merge quickly, at 80 Myrs, and their structure is still dense, unlike the merge product of eccentricity 0.5 at 180 Myrs in figure 3.5. The separation between the clusters decrease rapidly as we evolve them. With the merge event taking place at 80 Myrs, the distance between them is 0 for the rest of the simulation.

We plot the separation between the clusters center of mass over time comparing the graphs for different eccentricities in figure 3.7. We also compare the merge time for varying eccentricities and plot their orbital period in the same plot, seen in figure 3.9. The orbital period is calculated in accordance to Kepler's law

$$T = 2\pi\sqrt{\frac{a^3}{GM}},$$

where T is the orbital period, G the gravitational constant, M the mass of the cluster, a the semi-major axis of the cluster's orbit.

In the comparison between the half-mass radius of a single and a cluster within a binary, found in figure 3.8, we see that they both start at a half-mass radius of 1. Then as time passes, the increase in half-mass radius is quicker for the isolated star cluster, but ultimately they both display similar behavior. The irregular behavior which is more prominent in the isolated cluster could be due to the half-mass radius being affected to a large extent by escapers. If we had more stars within the cluster, we would see less of the irregular behavior as the effect of single stars escaping would have less of an impact on the total half-mass radius. As a star moves further from the center, but remain bound to the cluster, the half-mass radius increases. After it has escaped, the rest of the cluster which still is bound has a tighter half-mass radius, as the furthest away stars have escaped from the cluster. During the merge event of the cluster with eccentricity 0.0, we see a spike in the half-mass radius of the cluster. Since the clusters' internal structures still remain some time after the merge, the half-mass radius will increase before being seen following the same trend as before the merge.

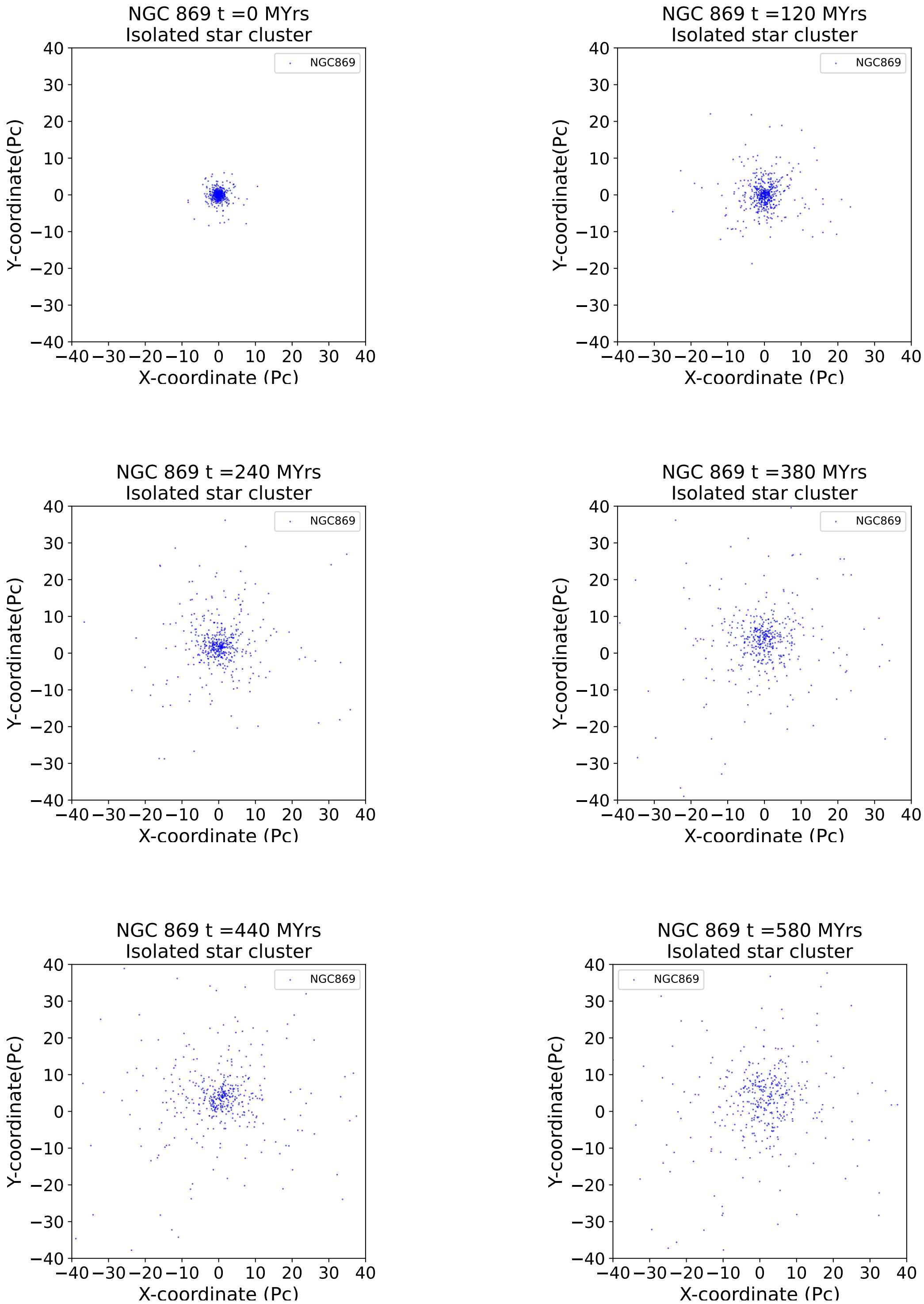

Figure 3.2: Time evolution of a single cluster.

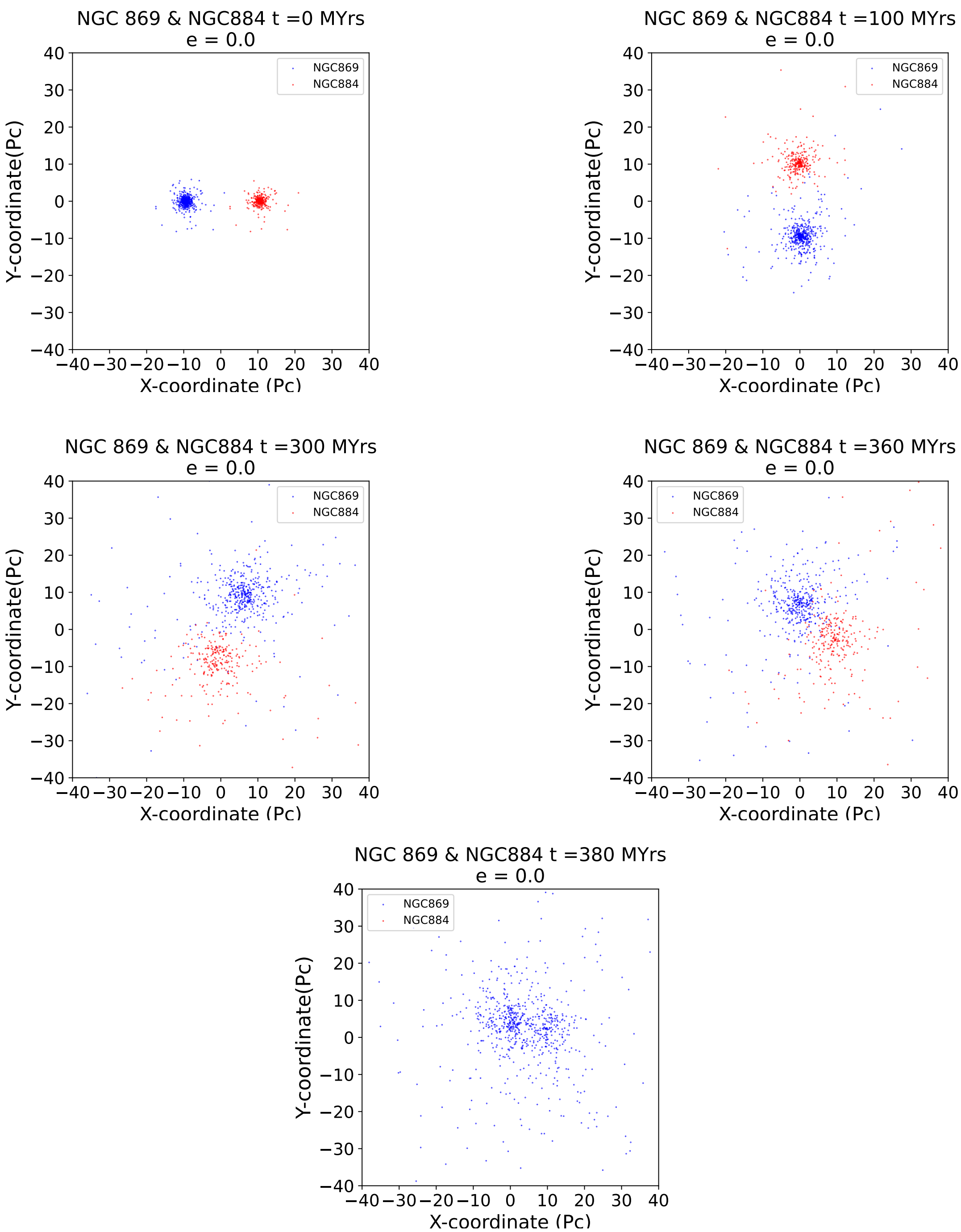

Figure 3.3: Time evolution for the double clusters with a circular orbit.

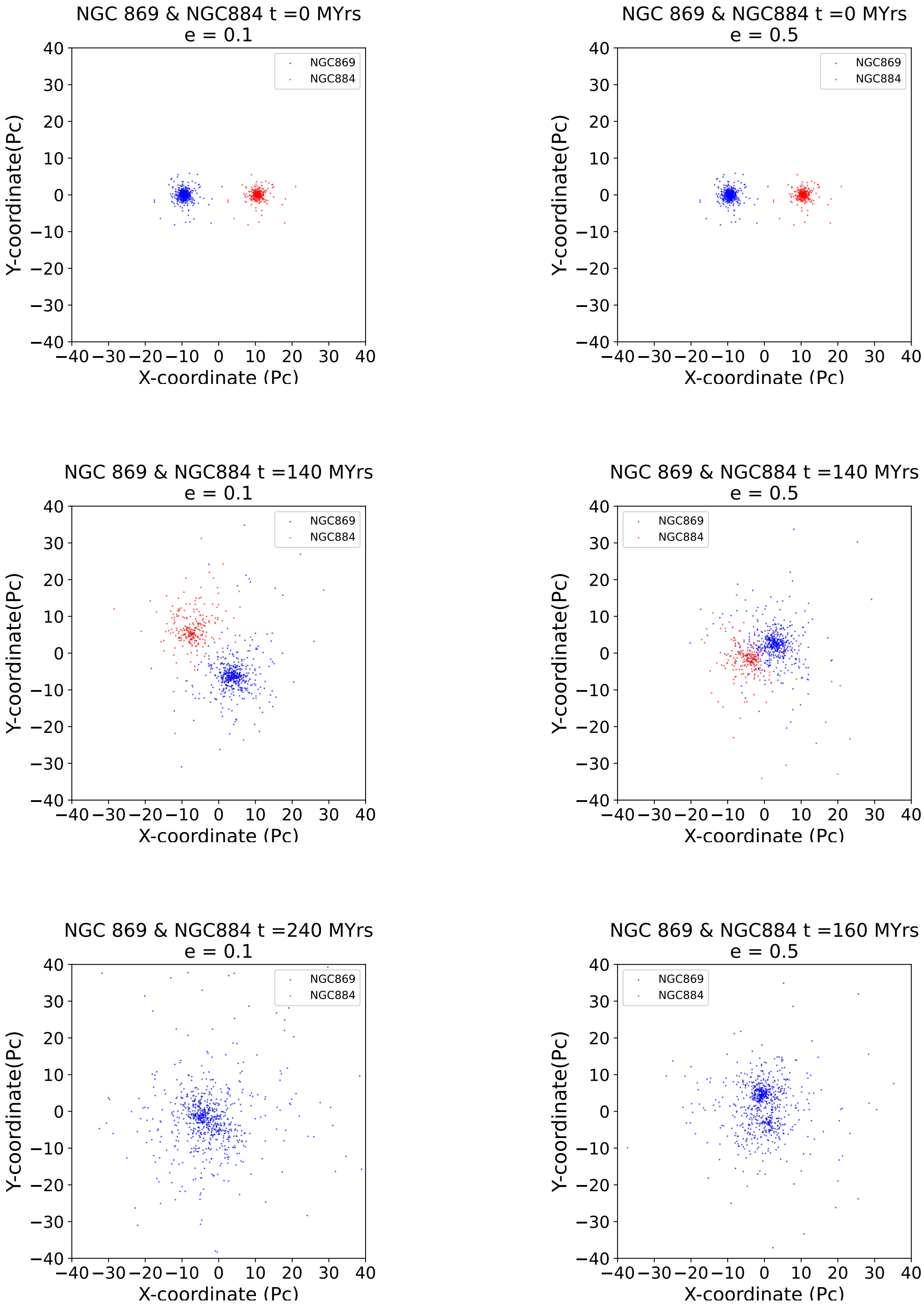

Figure 3.4: Time evolution of eccentricities 0.1 and 0.5 compared.

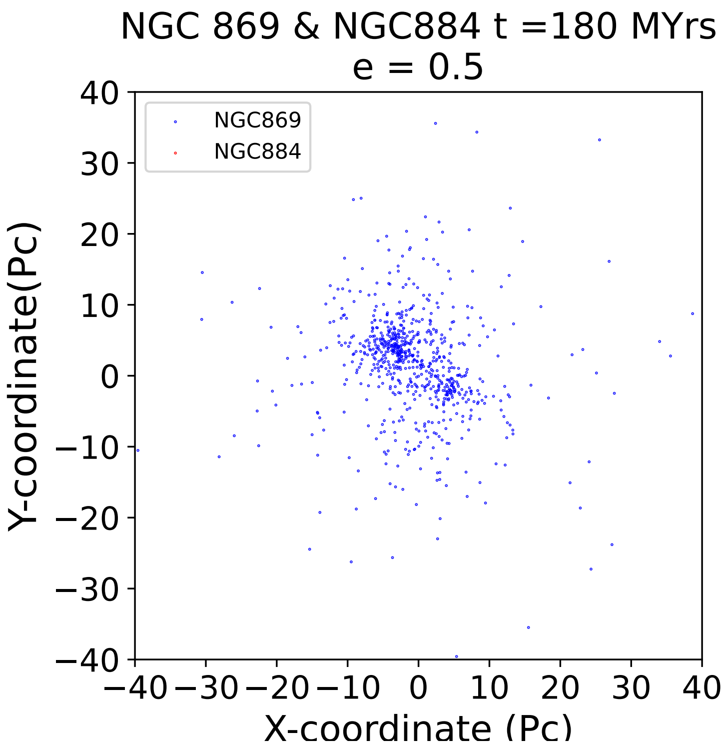

Figure 3.5: Further evolution of the clusters with initial eccentricity 0.5, at t = 180 Myrs.

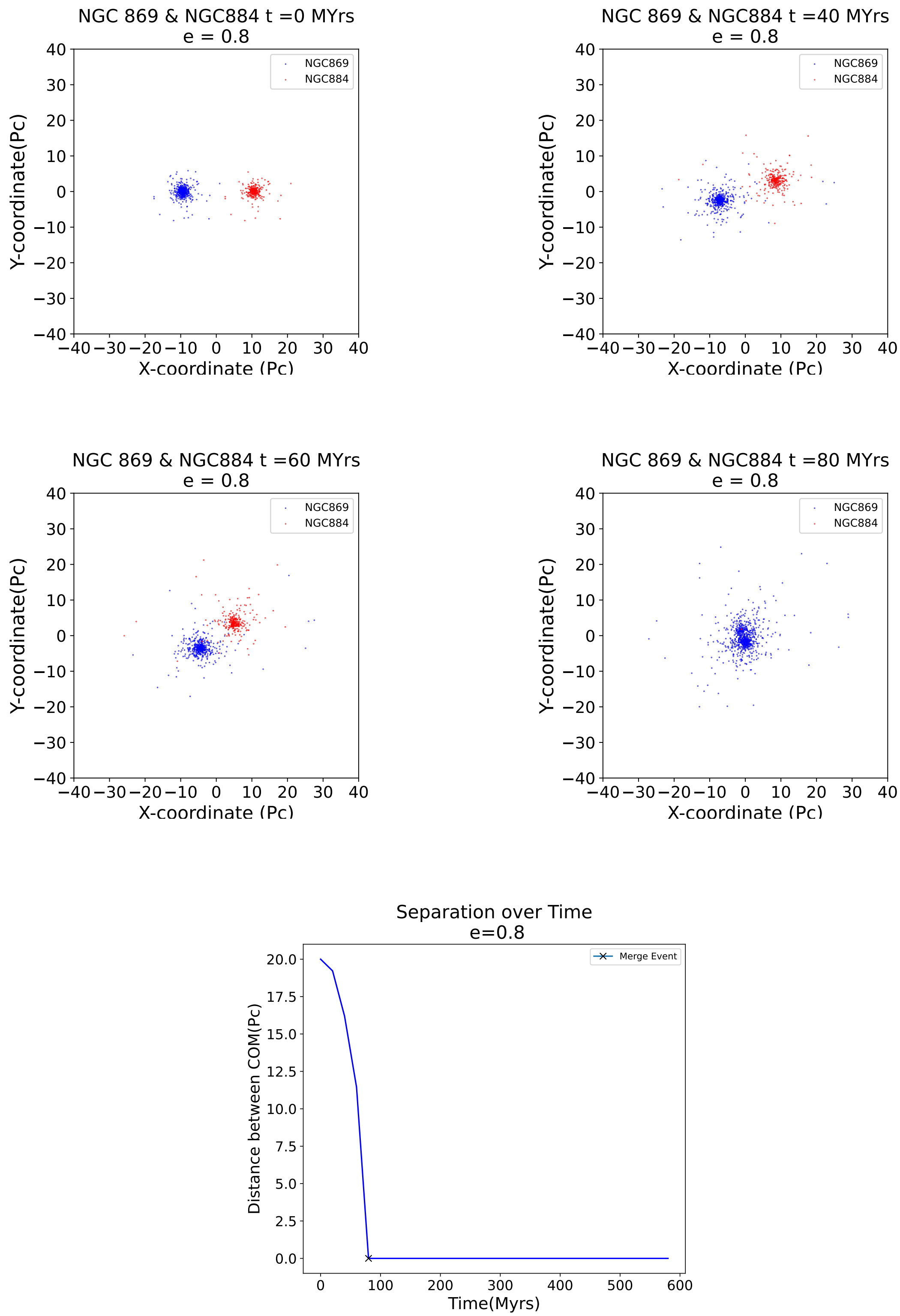

Figure 3.6: Time evolution of clusters with eccentricity 0.8. As well as the last image showing the distance between the cluster's centers of mass a function of time.

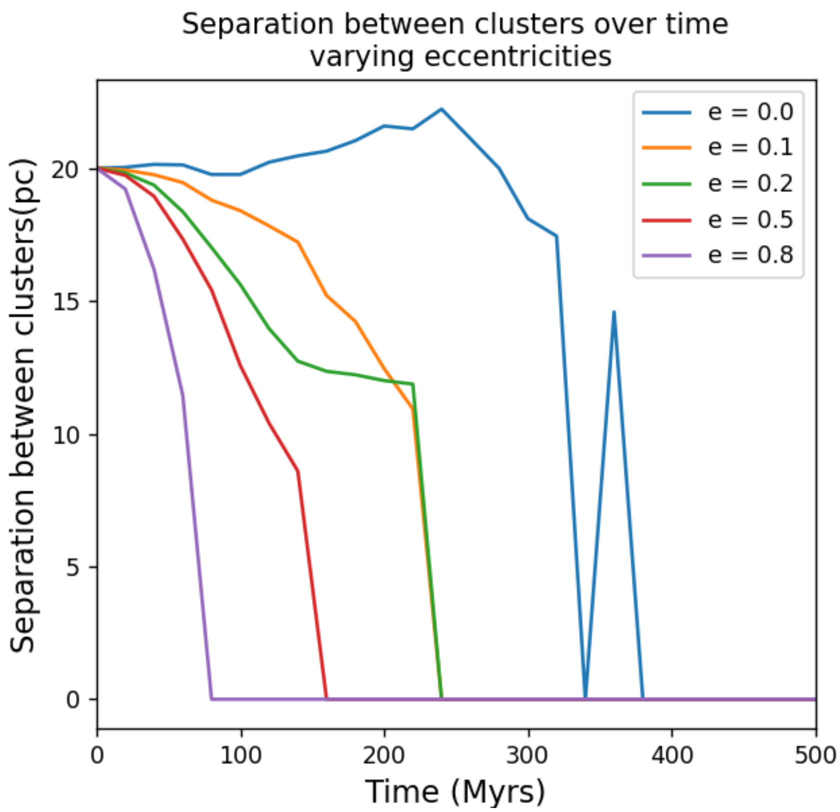

Figure 3.7: Varying eccentricities showing the distance between the clusters as a function of time.

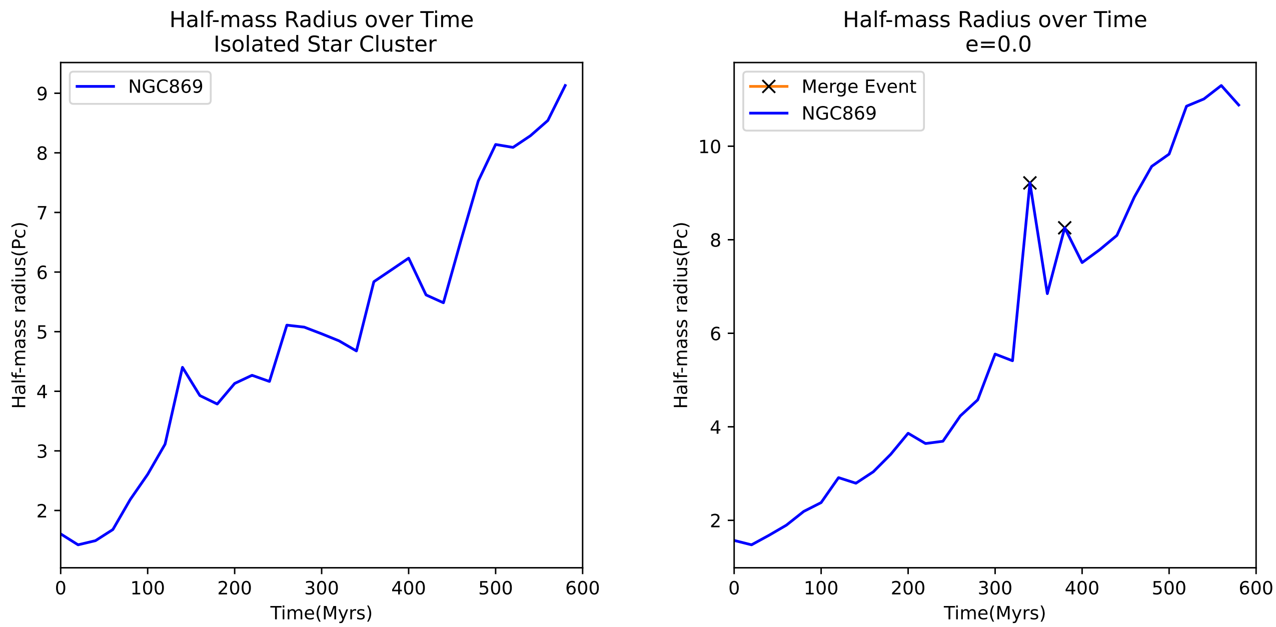

Figure 3.8: An isolated star clusters' half-mass radius over time compared to a cluster within a binary with eccentricity 0.0.

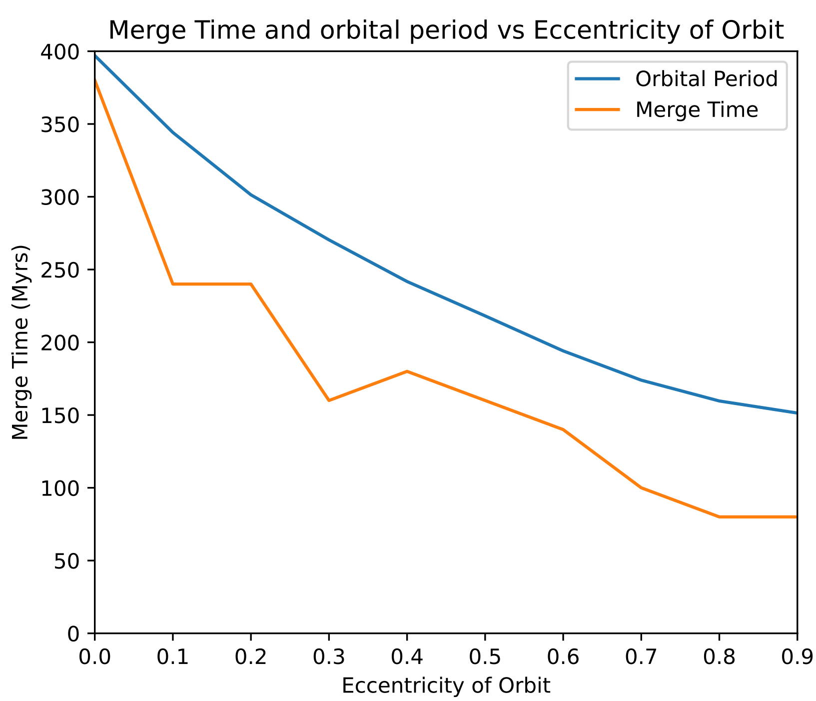

Figure 3.9: Merge time and orbital period for all eccentricities.

Chapter 4

Discussion

4.1 Eccentricity's effect on Merge-time

Our simulations on the clusters predict that these they will merge within 400 Myrs, due to the orbital energy between the clusters being transferred to the stars instead. We clearly see the effect that eccentricity of orbit has on the merge time for the clusters. The simulations with $e = 0.5$ shows that the merge time for the clusters are $\sim$ 80Myrs as seen in figure 3.4. For a completely circular orbit, the merge time is 380 Myrs as can be seen in figure 3.3. After this point, the stars within the clusters are shared between the initial clusters. The simulations with higher eccentricity for the clusters show a decreasing merge time for the clusters, with the exception of a point in merge time of $e = 0.4$, as shown in figure 3.9. This point is most likely a random fluctuation of the system as it is highly chaotic. Once the clusters have merged, they are no longer a double cluster. The merge time is found to follow a similar trend to the orbital period, with a larger difference between the two for a higher eccentricity.

Even for the circular orbit of eccentricity 0, the clusters merge relatively quickly in astronomical time-scales. We have found that for a double cluster with separation of 20 pc, such as the cluster NGC869 and NGC884, with a perfectly circular orbit, and no tidal disruption, the life-time is limited to around 400 Myrs before the clusters merge. An increasing eccentricity only leads to a shorter life-time for the clusters, which on every simulation merges within this time. In figure 3.4, in the last image of the cluster with eccentricity 0.5, the clusters still have a distinct shape. However, with our classification of the membership, all stars are bound to the same center of mass. One could possibly alter this classification to account for the structure within the clusters, in order to investigate the exact time the clusters merge. On the other hand, if we evolve this cluster further, as shown in figure 3.5 we can see that at 340 Myrs the cluster definitely is merged, so the roof value of 400 Myrs for life-time still holds even though the precise merge time could be altered within the script used for the analysis.

In this project we wanted to study an existing double cluster, with separation values available from real data, however in further research the experiment can be set up with varying separations as well. Increasing the separation would most likely increase the merge time and thus also the life-time of the clusters. What could then potentially limit the clusters life is how fast it evaporates due to processes within the cluster. A simulation of a single cluster can be seen in figure 3.2. This simulation uses the data for NGC 869, with 500 members and the same mean value for the stellar masses 0.5 solar mass, as for the previous runs. The half-mass radius of the cluster of the isolated cluster increases relatively linearly for the first 100 Myrs, as can be seen in the comparison in figure 3.8, then it reaches a peak at around 140 Myrs. If we look at the snapshots for this cluster, found in figures 3.2, we can see the cluster is evaporating over time. So for a single cluster with 500 members, we expect the half-mass radius to increase over time, as the cluster becomes more loosely bound as it loses stars due to natural processes within the cluster. Figure 3.8 shows that the cluster that is isolated follows a linear increasing trend, but displays some fluctuations due to the few number of stars within the cluster. This would cause the half-mass radius to be more sensitive to single stars escaping. The cluster within a binary with eccentricity 0.0 has a spike in half-mass radius as it merges, which is due to the internal structure of the separate clusters still being intact, even though they are now gravitationally bound into one cluster. We see two merge events on this run, most likely due to the script used, when some parts of the star cluster are bound together momentarily but later unbound. This does not last long as the cluster then becomes fully bound at $t = 380$ Myrs and does not separate again.

Still looking at figure 3.8, the increase in half-mass radius after the merge looks similar to the rate before the merge, which implies that once merged, the cluster evaporates at the same rate that it did before. It also means that the merging of two clusters does not have an effect on the subsequent evolution of the individual clusters. For the single star cluster, there are spikes where the half-mass radius increases and decreases rapidly. This could be due to escapers from the cluster coming back, as we redo the membership for each star for each snapshot of the cluster. If they happen to be unbound for a period of time, but then get trapped again, they re-enter the cluster and could decrease the half-mass radius. Another explanation could be that when the more loosely bound stars, which are most likely the outermost stars, escape from the cluster, the half mass radius decreases. This escaping, and re-entering of members of the cluster would possibly be the cause of this behaviour. The comparison between the two plots show that the clusters display similar behaviour in the first 100 Myrs, however the later life of the single cluster is less stable, with the probable explanation of the escaper-stars. The star cluster part of the binary has a more stable increase in the half-mass radius even after the merge time. This could mean that the merge event made the clusters evaporation more stable, but there is no evidence to say that it would make the cluster evaporate any slower.

4.1.1 Lifetime

The age of the clusters given in Song et al. (2022), is much less than the merge-time and thus life-time we have found for the double clusters, which a sign that the results are reasonable and agree with observations. Our results also agree with findings from for example (Darma et al. 2021), who found that binary star clusters rarely exhibit long-term stability, and that binary star cluster with small separations result in mergers. They state that only about ~ 30 percent remain after $t = 50$ Myrs when the clusters are formed in the Milky Way. The short life-time we found for the cluster was at its height 400 Myrs. This short life-time could be the reason we see so few of the binary clusters today. For small clusters as the ones we simulated, the evaporation process also limits for how long of a window we have to observe the clusters before merging or evaporating. Even for a perfectly circular orbit, a cluster of the kind of NGC 869 and NGC884 would only survive 400 Myrs after their formation. A reason why the eccentricity of the orbit affects the merging time of the clusters is due to the proximity the star clusters will come during their orbit. If they orbit closer, the gravitational attraction between stars become large and wins over the kinetic energy.

4.2 Energy error tolerance

The accumulated error produced from the simulation was highest for the eccentricity 0.8, and represents the systematic drift in total energy of the system. For eccentricity 0.8 this was $DE_{tot} = 69$. Where $DE = \frac{\Delta E}{E}$. These are errors from all the parts of the system, from the physics within the clusters and the stars within them. It is difficult to look past large errors like these, but for simulating a system of this kind, the error will be large due to the approximations. Since we varied the random seed input, which alters the way mass and energy is distributed in the system initially, and this produced very similar results, this error would most likely not affect the different kind of results we would get from the program. For the other runs this was lower, $DE_{tot} < 1\%$.

4.3 Further Research and Improvements

With the aid of even faster computers and the discovery of new materials used in their components we could in the future carry out direct N-body simulations with more and more stars. However, there are a few issues with today's semiconductors regarding toxicity of the materials and down scaling of the components (Winsnes, Elliot 2024). Further research within this field would be helpful to reduce the computing time for simulations with millions of bodies.

We could also have researched the other clusters mentioned in the paper (Song et al. 2022), or we could have investigated the dynamics of the merger product in detail. For example how the rotation of the clusters compare with the merge product, and how the merge product could display ”flattening” due to the merge. Using this we could look for dynamics like these to notice star clusters which could have been products of a merger. We are also assuming the clusters have an apocenter of 20 pc, as we observe them at this distance, however the clusters could be in another part of their orbit, and thus have a different apocenter. Since we can only use available data for the cluster, we make this assumption.

4.4 Conclusion

In conclusion, our project investigated if the discrepancy in the number of predicted binary star clusters and the number of observed could be explained by a short life-time of binary star clusters. One of the question we wanted to research was how varying eccentricity affects the life-time of a double cluster, which we found to have a large impact. Basing the simulations on a known double cluster we changed the input eccentricity of the double clusters, and found that the clusters merge even for a circular orbit. We also found that the merge time for a completely circular orbit is 380 Myrs, and that for higher eccentricity, it decreases. The shortest life-time was found for the highest eccentricity of 0.9, here the clusters merged after only 80 Myrs. Comparing the results with data on the ages of the clusters show that they align, even for the highest eccentricity and that the relatively short life-time of double clusters are a possible cause for the very few of them we observe today.

We also compared the half-mass radius between an isolated cluster and a cluster within a double cluster and found that they display similar behavior, with the isolated cluster's half-mass radius increasing slightly quicker. We also concluded that the double cluster has a spike in its half-mass radius as it merges due to the internal structure of the previously separate clusters still remaining some time after the merge event.

4.5 Acknowledgements

I would first of all like to thank my amazing supervisor Ross Church for the opportunity to be part of this project and to conduct research on such an interesting subject, and for always being there to help with any question I could think of. Next I want to thank my mother and father for always supporting and helping me, especially my father who has helped me countless of hours during my physics studies. I would also like to thank all of my amazing friends and colleagues at Lund University. Studying physics is far from a walk in the park, but it definitely helps to have you all by my side to laugh with. I'm forever grateful to have had the opportunity to share the amazing journey that the last few years have been with you. An extra thanks goes out to Julia Gidner, Matilda Skantz, Melvin Tham, Elliot Winsnes, Claudia Skoglund, Benjamin Dahlén, Johan Holmberg, Viktor Lehmann, Johann Schmand, Eric Svensson, and Filip Gustavsson.

Bibliography

Aarseth, S. 2003a, Gravitational N-Body Simulations: Tools and Algorithms, Cambridge Monographs on Mathematical Physics (Cambridge: Cambridge University Press)

Aarseth, S. 2003b, NBODY6 User Manual, Institute of Astronomy, University of Cambridge, available: [ftp://ftp.ast.cam.ac.uk/pub/sverre/nbody6/man6.pdf]

Ahmad & Cohen. 1973, Journal of Computational Physics, 12, 389

Bhatia, R. K. & Hatzidimitriou, D. 1988, MNRAS, 230, 215

Cantat-Gaudin & Anders, F. 2020, Astronomy and Astrophysics, 633, A99

Darma, R., Arifyanto, M. I., & Kouwenhoven, M. B. N. 2021, Monthly Notices of the Royal Astronomical Society, 506, 4603

de la Fuente Marcos, R. & de la Fuente Marcos, C. 2009, Astronomy and Astrophysics, 500, L13–L16

Hatzidimitriou, D. & Bhatia, R. K. 1990, Astronomy and Astrophysics, 230, 11

Heggie & Hut. 2003, The Gravitational Million-Body Problem (University of Edinburgh, Edinburgh and Institute for Advanced Study, Princeton)

Kharchenko, Piskunov, A. E., Schilbach, E., Röser, S., & Scholz, R.-D. 2012, AA, 543, A156

Krause, Offner, Charbonnel, et al. 2020, Space Science Reviews, 216

Kustaanheimo, SCHINZEL, DAVENPORT, & STIEFEL. 1965, Journal für die reine und angewandte Mathematik, 1965, 204

Pietrzynski, G. & Udalski, A. 2000, Acta Astronomica, 50, 337

Plummer. 1911, Monthly Notices of the Royal Astronomical Society, 71, 460

Rappenglück, M. A. 1999, Earth, Moon, and Planets, 85, 391

Song, Esamdin, Ali, Hu, Qingshun, & Zhang, Mengfan. 2022, AA, 666, A75

Vázquez, Moitinho, A., Carraro, G., & Dias, W. S. 2010, Astronomy and Astrophysics, 511, A38

Winsnes, Elliot. 2024, Structural analysis of HZO thin film and electrode using X-ray diffraction, Student Paper